Cooperative Spectrum Sensing with Secondary User Selection for Cognitive Radio Networks over Nakagami-m Fading Channels

Quoc-Tuan Vien, Huan X. Nguyen, and Arumugam Nallanathan

Abstract

This paper investigates cooperative spectrum sensing (CSS) in cognitive wireless radio networks (CWRNs). A practical system is considered where all channels experience Nakagami-m fading and suffer from background noise. The realisation of the CSS can follow two approaches where the final spectrum decision is based on either only the global decision at fusion centre (FC) or both decisions from the FC and secondary user (SU). By deriving closed-form expressions and bounds of missed detection probability (MDP) and false alarm probability (FAP), we are able to not only demonstrate the impacts of the m-parameter on the sensing performance but also evaluate and compare the effectiveness of the two CSS schemes with respect to various fading parameters and the number of SUs. It is interestingly noticed that a smaller number of SUs could be selected to achieve the lower bound of the MDP rather using all the available SUs while still maintaining a low FAP. As a second contribution, we propose a secondary user selection algorithm for the CSS to find the optimised number of SUs for lower complexity and reduced power consumption. Finally, numerical results are provided to demonstrate the findings.

Q.-T. Vien and H. X. Nguyen are with the Middlesex University, United Kingdom. Email: {q.vien; h.nguyen}@mdx.ac.uk.

A. Nallanathan is with the King's College London, United Kingdom. Email: arumugam.nallanathan@kcl.ac.uk.

Index Terms

Cognitive radio, cooperative spectrum sensing, user selection, Nakagami-m fading.

I. INTRODUCTION

Cognitive radio (CR) has recently emerged as a novel technology to efficiently exploit spectrum resource by implementing dynamic spectrum access [1], [2]. The secondary users (SUs) can opportunistically utilise the licenced frequency bands of the primary users (PUs) when they are not occupied. Thus, spectrum sensing is a basic element required at the SUs to detect the occupation and reappearance of the PUs [3]. Incorporating relaying techniques in cognitive wireless radio networks (CWRNs), cooperative spectrum sensing (CSS) has been proposed not only to help the shadowed SUs detect the licenced frequency bands but also to improve sensing reliability of the SUs [4]–[9].

Basically, a CSS scheme consists of sensing (SS) phase, reporting (RP) phase and backward (BW) phase. Every SU performs local spectrum sensing (LSS) to determine the availability of the licenced spectrum in the SS phase and then forwards its local decisions to a fusion centre (FC) in the RP phase. Collecting all LSS decisions, global spectrum sensing (GSS) is then carried out at the FC to make a global decision on the spectrum availability, which is then broadcast back to all the SUs in the BW phase.

In order to save the energy consumption of CSS in CWRNs, user selection approaches have been investigated in various works, such as [10]–[15]. Specifically, an energy-based user selection algorithm was proposed in [10] given battery life constraints of SUs. To deal with the dynamic changes of the network topology and channel conditions, a correlation-aware distributed user selection algorithm was developed in [11] to adaptively select the uncorrelated SUs for the CSS.

The overhead energy caused by the CSS was also dealt with in [12] where an energy-efficient node selection was proposed to select the best node based on the binary knapsack problem. In [13], the selection of sensing nodes can also be realised by linearly weighting the sensing data at all sensing nodes. Considering the scenario when only partial information of SUs and PUs is available in the wireless sensor networks, an energy-efficient sensor selection algorithm has been proposed in [14] to minimise the energy consumption while still satisfying the average detection probability. An optimisation framework has also been developed in [15] to solve the problem of joint sensing node selection, decision node selection and energy detection threshold aiming at saving energy consumption in cognitive sensor networks.

In this paper, we first analyse the probabilities of missed detection and false alarm of two CSS schemes over Nakagami-m fading channels, including i) *Global decision based CSS (GCSS)*: The GSS decision is the final spectrum sensing (FSS) decision at the SUs (e.g. [5]) and ii) *Mixture of local and global decisions based CSS (MCSS)*: Both the LSS and GSS decisions are taken into account to make the FSS decision at the SUs (e.g. [9]). In particular, we consider a practical scenario where all SS, RP and BW links suffer from fading and noises. Our work neither assumes the RP/BW channels are error-free [4], [5], [7], [12]. nor impractically requires instantaneous signal-to-noise ratio (SNR) information and excessive overhead [16], [17]. Our scheme requires a minimal 1-bit overhead for the report and feedback of sensing decisions. While a general criteria for decision-approach selection has been analytically derived in the presence of realistic channel propagation effects in [18], our work specifically aims at analysing and understanding behaviour of sensing performance over Nakagami-m channel with minimal overhead.

By deriving closed-form expressions of missed detection probability (MDP) and false alarm probability (FAP), we first compare the sensing performance achieved with the above CSS schemes and evaluate the effects of the number of SUs and the fading channel parameters on the performance. It is observed that GCSS scheme achieves a lower FAP while MCSS schemes improves the MDP. The fading parameters of the RP and BW channels are shown to have effects on both the MDP and FAP, while those of the SS channels only affect the MDP. Furthermore, the bounds of the MDP and FAP are then derived for a large number of SUs, which allows us to develop a secondary user selection algorithm for reducing the complexity and power consumption in the CSS.

The rest of the paper is organised as follows. In Section II, we introduce the system model of CWRNs and the process of GCSS and MCSS schemes. Section III derives the expressions and bounds of FAP and MDP for both CSS schemes over Nakagami-m fading channels. The secondary user selection algorithm for the CSS is presented in Section IV. Numerical results are presented and discussed in Section V. Finally, Section VI concludes the paper.

II. System Model & Cooperative Spectrum Sensing

A. System Model

The system model of a CWRN under investigation is illustrated in Fig. 1 consisting of $\mathcal{PU}$, $\{\mathcal{SU}_1, \mathcal{SU}_2, \ldots, \mathcal{SU}_N\}$ and $\mathcal{FC}$. We assume there are K non-overlapping licenced frequency bands $f_1, f_2, \ldots, f_K$. Two hypothesis that the k-th frequency band is occupied and unoccupied by $\mathcal{PU}$ are denoted by $\mathcal{H}_{1,k}$ and $\mathcal{H}_{0,k}$, respectively. For convenience, let us define a spectrum indicator vector (SIV) $\mathrm{s}_A^{(M)}$, $M \in \{L, G, F_j\}$, $A \in \{SU_i, FC\}$, $i = 1, 2, \ldots, N$, $j = 1, 2$, of length K (in bits) to report the availability of the licenced spectrum in the LSS at $\mathcal{SU}_i$, the GSS at $\mathcal{FC}$ and the FSS at $\mathcal{SU}_i$ using scheme j. The unavailable and available frequency bands

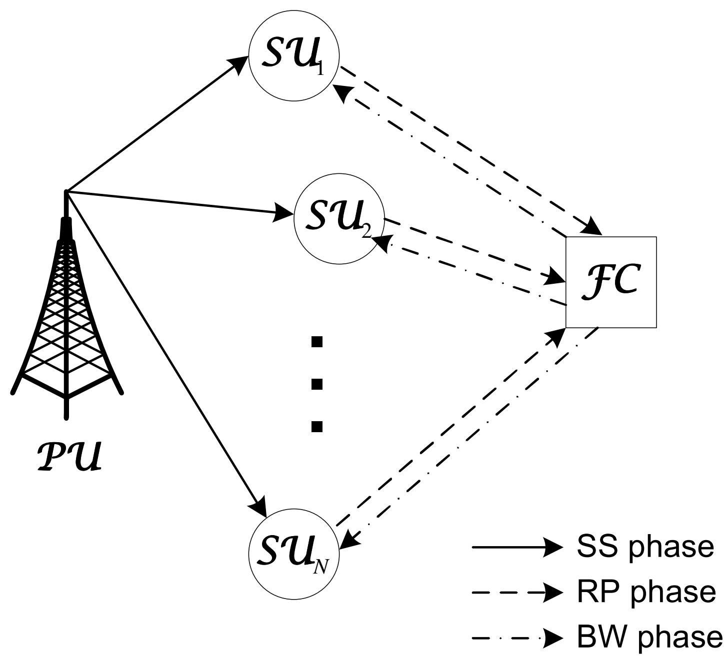

Fig. 1: System model of cognitive wireless relay network.

are represented in $\mathbf{s}_A^{(M)}$ by bits '0' and '1', respectively. The channel for a link $\mathcal{A}_1 \to \mathcal{A}_2$ is denoted by $h_{A_1A_2}$, $\{A_1, A_2\} \in \{P, S_i, F\}$, $A_1 \neq A_2$, and assumed to suffer from quasi-static slow Nakagami-m fading. Complex Gaussian noise vector $\mathbf{n}_A^{(T)}$, $T \in \{SS, RP, BW\}$, is assumed at receiver node A in phase T, in which each entry has zero mean and variance of σ_0^2.

B. Cooperative Spectrum Sensing (CSS)

Three phases of CSS can be briefly described as follows:

1) Sensing (SS) Phase - Local Spectrum Sensing (LSS): The signal sensed at $\mathcal{SU}_i$, $i = 1, 2, \ldots, N$, at f_k, $k = 1, 2, \ldots, K$, can be expressed as

$$\mathbf{r}_{SU_i}^{(SS)}[k] = \begin{cases} h_{PS_i}\mathbf{x}[k] + \mathbf{n}_{SU_i}^{(SS)}[k], & \mathcal{H}_{1,k}, \\ \mathbf{n}_{SU_i}^{(SS)}[k], & \mathcal{H}_{0,k}, \end{cases} \tag{1}$$

where $\mathbf{x}[k]$ is the transmitted signal from $\mathcal{PU}$. Then, $\mathcal{SU}_i$ detects the availability of f_k by comparing the energy of the received signal in (1) with an energy threshold $\varepsilon_i[k]$ via an energy measurement $\xi[\cdot]$ as follows:

$$\mathbf{s}_{SU_i}^{(L)}[k] = \begin{cases} 0, & \text{if } \xi[\mathbf{r}_{SU_i}^{(SS)}[k]] \geqslant \varepsilon_i[k], \\ 1, & \text{otherwise.} \end{cases} \tag{2}$$

2) Reporting (RP) Phase - Global Spectrum Sensing (GSS): The received signal at $\mathcal{FC}$ from $\mathcal{SU}_i$, $i = 1, 2, \ldots, N$, at f_k, $k = 1, 2, \ldots, K$, can be written by

$$\mathbf{r}_i^{(RP)}[k] = \sqrt{\Lambda_i} h_{S_i F} \mathbf{x}_{SU_i}^{(L)}[k] + \mathbf{n}_{FC}^{(RP)}[k], \tag{3}$$

where Λ_i is the transmission power of $\mathcal{SU}_i$ and $\mathbf{x}_{SU_i}^{(L)}[k]$ is the binary phase shift keying (BPSK) modulated version of $\mathbf{s}_{SU_i}^{(L)}[k]$ (see (2)). Then, $\mathcal{FC}$ decodes and combines all the decoded SIVs (denoted by $\{\mathbf{s}_i^{(RP)}[k]\}$) from all $\{\mathcal{SU}_i\}$ using the OR rule to make a global decision as

$$\mathbf{s}_{FC}^{(G)}[k] = \begin{cases} 0, & \text{if } \sum_{i=1}^{N} \mathbf{s}_i^{(RP)}[k] < N, \\ 1, & \text{otherwise.} \end{cases} \tag{4}$$

3) Backward (BW) Phase - Final Spectrum Sensing (FSS): The received signal at $\mathcal{SU}_i$, $i = 1, 2, \ldots, N$, from $\mathcal{FC}$ with respect to f_k, $k = 1, 2, \ldots, K$, is given by

$$\mathbf{r}_{SU_i}^{(BW)}[k] = \sqrt{\Lambda_{FC}} h_{FS_i} \mathbf{x}_{FC}^{(G)}[k] + \mathbf{n}_{SU_i}^{(BW)}[k], \tag{5}$$

where Λ_{FC} is the transmission power of $\mathcal{FC}$ and $\mathbf{x}_{FC}^{(G)}[k]$ is the BPSK modulated version of $\mathbf{s}_{FC}^{(G)}[k]$ (see (4)). Then, $\mathcal{SU}_i$ decodes the received signal as $\mathbf{s}_{SU_i}^{(BW)}[k]$.

<u>*GCSS scheme*</u>: The GSS decision received from $\mathcal{FC}$ is also the FSS at $\mathcal{SU}_i$. Thus, we have

$$\mathbf{s}_{SU_i}^{(F_1)}[k] = \mathbf{s}_{SU_i}^{(BW)}[k]. \tag{6}$$

<u>*MCSS scheme*</u>: $\mathcal{SU}_i$ combines its local SIV with the global SIV received from $\mathcal{FC}$ as [9]:

$$\mathbf{s}_{SU_i}^{(F_2)}[k] = \begin{cases} 0, & \text{if } (\mathbf{s}_{SU_i}^{(L)}[k] + \mathbf{s}_{SU_i}^{(BW)}[k]) < 2, \\ 1, & \text{otherwise.} \end{cases} \tag{7}$$

III. Performance Analysis

In this section, we analyse the FAP and MDP of two CSS schemes. Without loss of generality, a specific frequency band is considered and thus the index of the frequency band (i.e. k) is omitted in the rest of the letter. The Nakagami fading parameters of the SS, RP and BW channels are denoted by m_{ss}, m_{rp} and m_{bw}, respectively. We assume that the RP and BW channels of the same link have the same Nakagami fading parameters (i.e. $m_{rp} = m_{bw}$) and all the SUs have the same energy threshold (i.e. $\varepsilon_i[k] = \varepsilon[k]\ \forall i = 1, 2, \ldots, N$).

Define $\alpha \triangleq \varepsilon/(2\sigma_0^2)$ and $\beta_i \triangleq m_{ss}\sigma_0^2/(m_{ss}\sigma_0^2 + \gamma_{PS_i})$, $i = 1, 2, \ldots, N$, where γ_{PS_i} is the average SNR at $\mathcal{SU}_i$ over h_{PS_i}. The FAP and MDP of the LSS are given by [19]

$$P_f^{(SU_i)} = \Pr\{s_{SU_i}^{(L)} = 0|\mathcal{H}_0\} = \frac{\Gamma_u(\rho, \alpha)}{\Gamma(\rho)}, \tag{8}$$

$$P_m^{(SU_i)} = \Pr\{s_{SU_i}^{(L)} = 1|\mathcal{H}_1\} = 1 - \vartheta_{i,1} - \vartheta_{i,2}, \tag{9}$$

where

$$\vartheta_{i,1} = e^{\left(-\frac{\alpha\beta_i}{m_{ss}}\right)}[\beta_i^{m_{ss}-1} L_{m_{ss}-1}(-\alpha(1-\beta_i)) + (1-\beta_i)\sum_{j=0}^{m_{ss}-2} \beta_i^j L_j(-\alpha(1-\beta_i))], \tag{10}$$

$$\vartheta_{i,2} = \beta_i^{m_{ss}} e^{-\alpha} \sum_{j=1}^{\rho-1} \frac{\alpha^j}{j!} {}_1F_1(m_{ss}; j+1; \alpha(1-\beta_i)), \tag{11}$$

ρ denotes the time-bandwidth product of the energy detector, $\Gamma(\cdot)$ is the gamma function [20, eq. (8.310.1)], $\Gamma_u(\cdot,\cdot)$ is the upper incomplete gamma function [20, eq. (8.350.2)], ${}_1F_1(\cdot;\cdot;\cdot)$ is the confluent hypergeometric function [20, eq. (9.210.1)] and $L_i(\cdot)$ is the Laguerre polynomial of degree i [20, eq. (8.970.2)].

Over a Nakagami-m fading channel h_{AB}, the average bit error rate (BER) for BPSK modulation with respect to the average SNR of γ_{AB} is obtained as in [21] and given below

$$P_b(E_{AB}) = \left(1 + \frac{\gamma_{AB}}{m_{AB}}\right)^{-m_{AB}} \frac{\Gamma(m_{AB} + 1/2)}{2\sqrt{\pi}\Gamma(m_{AB} + 1)} {}_2F_1(m_{AB}, 1/2; m_{AB} + 1; 1/(1 + \gamma_{AB}/m_{AB}))$$
$$\triangleq \psi_{AB}, \tag{12}$$

where ${}_2F_1(\cdot, \cdot; \cdot; \cdot)$ is the Gauss hypergeometric function [20, eq. (9.100)].

Considering the GSS at $\mathcal{FC}$, we obtain the following:

Lemma 1. *The FAP and MDP of the GSS are determined by*

$$P_f^{(FC)} = 1 - \frac{1}{[\Gamma(\rho)]^N} \prod_{i=1}^{N} [\Gamma_l(\rho, \alpha)(1 - \psi_{S_iF}) + \Gamma_u(\rho, \alpha)\psi_{S_iF}], \tag{13}$$

$$P_m^{(FC)} = \prod_{i=1}^{N} [(1 - \vartheta_{i,1} - \vartheta_{i,2})(1 - \psi_{S_iF}) + (\vartheta_{i,1} + \vartheta_{i,2})\psi_{S_iF}], \tag{14}$$

where ψ_{S_iF} is given by (12) *and $\Gamma_l(\cdot, \cdot)$ is the lower incomplete gamma function [20, eq. (8.350.1)].*

Proof: From (4), the FAP and MDP at $\mathcal{FC}$ are given by

$$P_f^{(FC)} = \Pr\{s_{FC}^{(G)} = 0|\mathcal{H}_0\} = 1 - \prod_{i=1}^{N} \Pr\{s_i^{(RP)} = 1|x = 0\}, \tag{15}$$

$$P_m^{(FC)} = \Pr\{s_{FC}^{(G)} = 1|\mathcal{H}_1\} = \prod_{i=1}^{N} \Pr\{s_i^{(RP)} = 1|x \neq 0\}. \tag{16}$$

Thus, over the Nakagami-m fading RP channels, we have

$$P_f^{(FC)} = 1 - \prod_{i=1}^{N} [(1 - P_f^{(SU_i)})(1 - \psi_{S_iF}) + P_f^{(SU_i)}\psi_{S_iF}], \tag{17}$$

$$P_m^{(FC)} = \prod_{i=1}^{N} [P_m^{(SU_i)}(1 - \psi_{S_iF}) + (1 - P_m^{(SU_i)})\psi_{S_iF}]. \tag{18}$$

Substituting (8) and (9) into (17) and (18) with the fact $\Gamma_u(\rho,\alpha)+\Gamma_l(\rho,\alpha)=\Gamma(\rho)$ [20, eq. (8.356.3)], the lemma is proved. ■

In the BW phase, we have the following findings:

Lemma 2. *The FAP and MDP of the FSS at $\mathcal{SU}_i$, $i=1,2,\ldots,N$, using GCSS scheme are determined by*

$$P_{f,1}^{(SU_i)}=1-[(1-P_f^{(FC)})(1-\psi_{FS_i})+P_f^{(FC)}\psi_{FS_i}], \tag{19}$$

$$P_{m,1}^{(SU_i)}=P_m^{(FC)}(1-\psi_{FS_i})+(1-P_m^{(FC)})\psi_{FS_i}. \tag{20}$$

Proof: From (6), the proof can be straightforwardly obtained as in Lemma 1. ■

Lemma 3. *The FAP and MDP of the FSS at $\mathcal{SU}_i$, $i=1,2,\ldots,N$, using MCSS scheme are determined by*

$$P_{f,2}^{(SU_i)}=1-\frac{1}{\Gamma(\rho)}[\Gamma_l(\rho,\alpha)(1-\psi_{FS_i})+\Gamma_u(\rho,\alpha)\psi_{FS_i}][(1-P_f^{(FC)})(1-\psi_{FS_i})+P_f^{(FC)}\psi_{FS_i}], \tag{21}$$

$$P_{m,2}^{(SU_i)}=[(1-\vartheta_{i,1}-\vartheta_{i,2})(1-\psi_{FS_i})+(\vartheta_{i,1}+\vartheta_{i,2})\psi_{FS_i}][P_m^{(FC)}(1-\psi_{FS_i})+(1-P_m^{(FC)})\psi_{FS_i}]. \tag{22}$$

Proof: From (7), $P_{f,2}^{(SU_i)}$ and $P_{m,2}^{(SU_i)}$ can be given by

$$P_{f,2}^{(SU_i)}=\Pr\{s_{SU_i}^{(F_2)}=0|\mathcal{H}_0\}=1-\Pr\{s_{SU_i}^{(L)}=1|x=0\}\Pr\{s_{SU_i}^{(BW)}=1|x=0\}, \tag{23}$$

$$P_{m,2}^{(SU_i)}=\Pr\{s_{SU_i}^{(F_2)}=1|\mathcal{H}_1\}=\Pr\{s_{SU_i}^{(L)}=1|x\neq 0\}\Pr\{s_{SU_i}^{(BW)}=1|x\neq 0\}. \tag{24}$$

Thus, over the Nakagami-m BW channels h_{FS_i}, $P_{f,2}^{(SU_i)}$ and $P_{m,2}^{(SU_i)}$ can be obtained by (21) and (22), respectively. ■

Remark 1 (*Lower FAP with GCSS scheme and Lower MDP with MCSS scheme*)**.** From (19), (20), (21) and (22) in Lemmas 2 and 3, it can be easily shown that $P_{f,1}^{(SU_i)}<P_{f,2}^{(SU_i)}$ and

$P_{m,1}^{(SU_i)} > P_{m,2}^{(SU_i)}$, $i = 1, 2, \ldots, N$.

Remark 2 (*Lower MDP but Higher FAP with Increased Number of SUs*)**.** From (13) and (14) in Lemma 1, it can be seen that $P_f^{(FC)}$ and $P_m^{(FC)}$ monotonically increase and decrease, respectively, over N. Thus, from (19), (20), (21) and (22), the increased number of SUs helps both CSS schemes improve the MDP, however, causing a higher FAP.

Remark 3 (*Impact of Nakagami-m Fading Parameters on MDP and FAP*)**.** Both the MDP and FAP decrease when the fading parameters of RP and BW channels increase, while only MDP is improved with increased fading parameters of SS channels. In fact, it is known that the BER of a Nakagami-m fading channel h_{AB} monotonically decreases as m_{AB} increases (see (12)). Thus, from (19), (20), (21) and (22), it can be proved that $P_{f,j}^{(SU_i)}$ and $P_{m,j}^{(SU_i)}$, $i = 1, 2, \ldots, N$, $j = 1, 2$, monotonically decrease as either m_{rp} or m_{bw} increases. Additionally, as shown in (8) and (9), $P_f^{(SU_i)}$, $i = 1, 2, \ldots, N$, of the LSS is independent of m_{ss}, while a lower $P_m^{(SU_i)}$ is achieved as m_{ss} increases.

Bounds of FAPs and MDPs:

According to Remark 2, there is a significant impact of the number of SUs on FAPs and MDPs. For the sake of providing insightful meanings of the above derived expressions for the FAPs and MDPs of the two CSS schemes, let us investigate a specific scenario of identical channels, i.e. $\gamma_{PS_i} \triangleq \gamma_{ss}$, $\gamma_{S_iF} \triangleq \gamma_{rp}$, $\gamma_{FS_i} \triangleq \gamma_{bw}$, $\forall i = 1, 2, \ldots, N$. Thus, from (10) and (11), we can rewrite $\vartheta_{i,1} = \vartheta_1$ and $\vartheta_{i,2} = \vartheta_2$.

Lemma 4. *When the number of SUs is very large, i.e. $N \to \infty$, FAP and MDP of GCSS scheme* *approach* $P^{(SU)}_{f,1_{N_\infty}}$ *and* $P^{(SU)}_{m,1_{N_\infty}}$*, respectively, where*

$$P^{(SU)}_{f,1_{N_\infty}} = 1 - \psi_{bw}, \tag{25}$$

$$P^{(SU)}_{m,1_{N_\infty}} = \psi_{bw}. \tag{26}$$

Proof: As $N \to \infty$, from Lemma 1, it can be seen that $P_f^{(FC)} \to 1$ and $P_m^{(FC)} \to 0$. Substituting into (19) and (20), we obtain $P^{(SU)}_{f,1_{N_\infty}}$ and $P^{(SU)}_{m,1_{N_\infty}}$ as shown in (25) and (26). ■

Lemma 5. *When the number of SUs is very large, i.e.* $N \to \infty$*, FAP and MDP of MCSS scheme approach* $P^{(SU)}_{f,2_{N_\infty}}$ *and* $P^{(SU)}_{m,2_{N_\infty}}$*, respectively, where*

$$P^{(SU)}_{f,2_{N_\infty}} = 1 - \frac{\Gamma_l(\rho,\alpha)}{\Gamma(\rho)}\psi_{bw} - \frac{\Gamma_u(\rho,\alpha) - \Gamma_l(\rho,\alpha)}{\Gamma(\rho)}\psi_{bw}^2, \tag{27}$$

$$P^{(SU)}_{m,2_{N_\infty}} = (1 - \vartheta_1 - \vartheta_2)\psi_{bw} - (1 - 2\vartheta_1 - 2\vartheta_2)\psi_{bw}^2. \tag{28}$$

Proof: The proof is similarly obtained as in Lemma 4. ■

Remark 4 (*Lower MDP with MCSS scheme and Approximately Similar FAPs*)**.** In fact, from (26) and (28), it can be easily shown that $P^{(SU)}_{m,2_{N_\infty}} < P^{(SU)}_{m,1_{N_\infty}}$, which means that a lower MDP bound is achieved with MCSS scheme. Considering the FAP bound, it is noted that $\Gamma_l(\rho,\alpha) \approx \Gamma(\rho)$ as $\alpha = \varepsilon/(2\sigma_0^2) \to \infty$. Also, we have $\psi_{bw}^2 \ll \psi_{bw} < 1$. Thus, from (27), we have $P^{(SU)}_{f,2_{N_\infty}} \approx 1 - \psi_{bw} = P^{(SU)}_{f,1_{N_\infty}}$.

IV. Secondary User Selection for the CSS

From Lemmas 4 and 5, it is noted that, given a large number of available SUs for CSS, we can select a smaller number of SUs to achieve the lower bound of the MDP instead of using all the SUs while still guaranteeing an achievable lower FAP.

Let N_{opt} denote the optimised number of SUs for the CSS. We achieve the following:

Lemma 6. *The optimised number of SUs for the CSS is determined by*

$$N_{opt} = n \left| \sum_{k=0}^{n} \begin{pmatrix} n \\ k \end{pmatrix} (-1)^k \left[\psi_{rp} + (\vartheta_1 + \vartheta_2)(1 - 2\psi_{rp})\right]^k = \tau, \right. \tag{29}$$

where $\tau \to 0^+$ is an extremely small positive number.

Proof: In Lemmas 4 and 5, the lower bound of the MDP of Scheme j, $j = 1, 2$, i.e. $P^{(SU)}_{m,j_{N_\infty}}$, is achieved as $P^{(FC)}_m \to 0$.

From (14) with identical fading channels, the MDP of the GSS can be rewritten as

$$\begin{aligned} P^{(FC)}_m &= \left[\psi_{rp} + (1 - \vartheta_1 - \vartheta_2)(1 - 2\psi_{rp})\right]^N \\ &= \left[1 - \psi_{rp} - (\vartheta_1 + \vartheta_2)(1 - 2\psi_{rp})\right]^N. \end{aligned} \tag{30}$$

Applying Taylor expansion of power series [20, eq. (1.111)], we obtain

$$P^{(FC)}_m = \sum_{k=0}^{n} \begin{pmatrix} n \\ k \end{pmatrix} (-1)^k \left[\psi_{rp} + (\vartheta_1 + \vartheta_2)(1 - 2\psi_{rp})\right]^k. \tag{31}$$

Denote τ as an extremely small positive number, i.e. $\tau \to 0^+$. Since $P^{(FC)}_m \to 0$, the optimised number of SUs can be found by solving $P^{(FC)}_m = \tau$. The lemma is proved. ■

It is noted in Lemma 6 that N_{opt} can be determined using numerical method. A secondary user selection algorithm can thus be proposed as summarised in Table. I[1].

[1]Note that the determination of the optimised number of SUs and the user selection for the CSS can be carried out with the assistance of a coordinator, e.g. $\mathcal{FC}$.

TABLE I: Secondary user selection algorithm for the CSS

Given m_{ss}, m_{rp}, σ_0, γ_{ss}, γ_{rp}, ε, ρ, τ:
Step 1: Find ϑ_1, ϑ_2 and ψ_{rp} using (10), (11) and (12), respectively.
Step 2: Find N_{opt} in Lemma 6:
$n = 1$
while $n \leqslant N$ **do**
compute $S = \sum_{k=0}^{n} \begin{pmatrix} n \\ k \end{pmatrix} (-1)^k \left[\psi_{rp} + (\vartheta_1 + \vartheta_2)(1 - 2\psi_{rp})\right]^k$
if $S \leqslant \tau$ **then**
break
end if
$n = n + 1$
end while
$N_{opt} = n$
Step 3: Select N_{opt} among N available SUs based on their local sensing data (e.g. [7]).

V. Numerical Results

Fig. 2 shows the MDP against the FAP of two CSS schemes (i.e. FCSS and MCSS) with respect to various fading parameters and various values of the energy threshold. We assume there are 10 SUs (i.e. $N = 10$) and the time-bandwidth product of the energy detector is $\rho = 5$. The SNRs of the channels are set as follows: $\{\gamma_{PS_i}\} = \{10, 8, 9, 12, 5, 7, 8, 4, 2, 6\}$ dB, $\{\gamma_{S_iF}\} = \{8, 7, 10, 4, 6, 8, 9, 11, 8, 10\}$ dB and $\{\gamma_{FS_i}\} = \{10, 11, 13, 9, 8, 14, 11, 10, 12, 7\}$ dB. Two Nakagami-m fading scenarios are considered: i) $m_{ss} = 3$, $m_{rp} = m_{bw} = 1$ and ii) $m_{ss} = 1$, $m_{rp} = m_{bw} = 2$. It can be observed that, at a given energy threshold, the MCSS scheme achieves a lower MDP than the FCSS scheme, while a lower FAP is achieved with the FCSS compared to the MCSS. This observation confirms the statement in Remark 1. Additionally, the

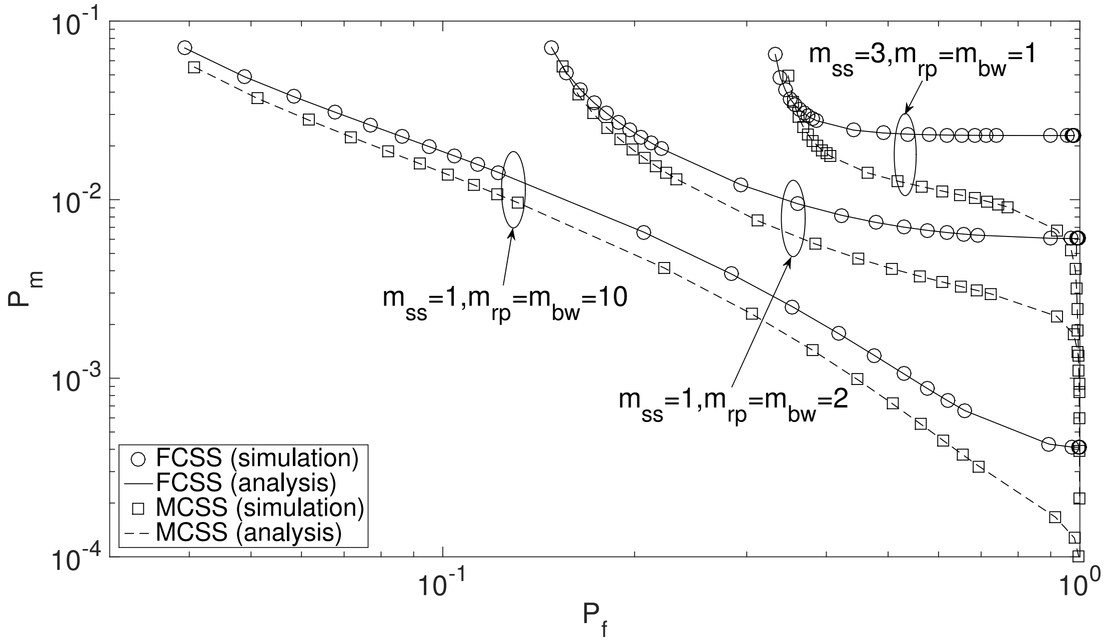

Fig. 2: Performance comparison of two CSS schemes.

analytical results of the FAP and MDP for both CSS schemes derived in Lemmas 2 and 3 are shown to be consistent with the simulation results.

Investigating the impact of Nakagami-m fading parameters on the sensing performance of the CSS, Fig. 3 plots the MDP versus FAP of MCSS scheme with respect to various fading scenarios[2]. A total of 10 SUs is considered and the SNRs of the SS, RP and BW channels are similarly set as in Fig. 2. As shown in Fig. 3, given fixed m_{ss}, both the MDP and FAP are improved as m_{rp} (or m_{bw}) increases. Considering the scenario of fixed m_{rp} and m_{bw}, a lower MDP is achieved as m_{ss} increases, while the FAP is unchanged for all values of the energy threshold. These above comparisons verify the statement in Remark 3.

The impact of the number of SUs on the sensing performance of various CSS schemes is

[2]The impact of the fading parameters on the sensing performance of GCSS scheme can be similarly observed, and thus is omitted for brevity.

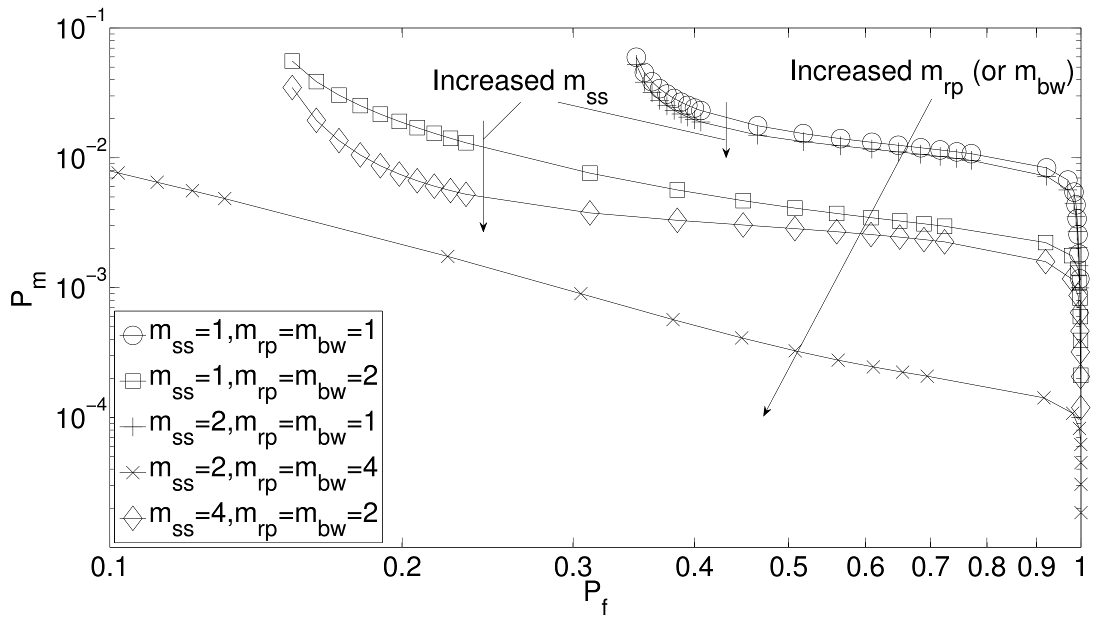

Fig. 3: Performance of MCSS scheme.

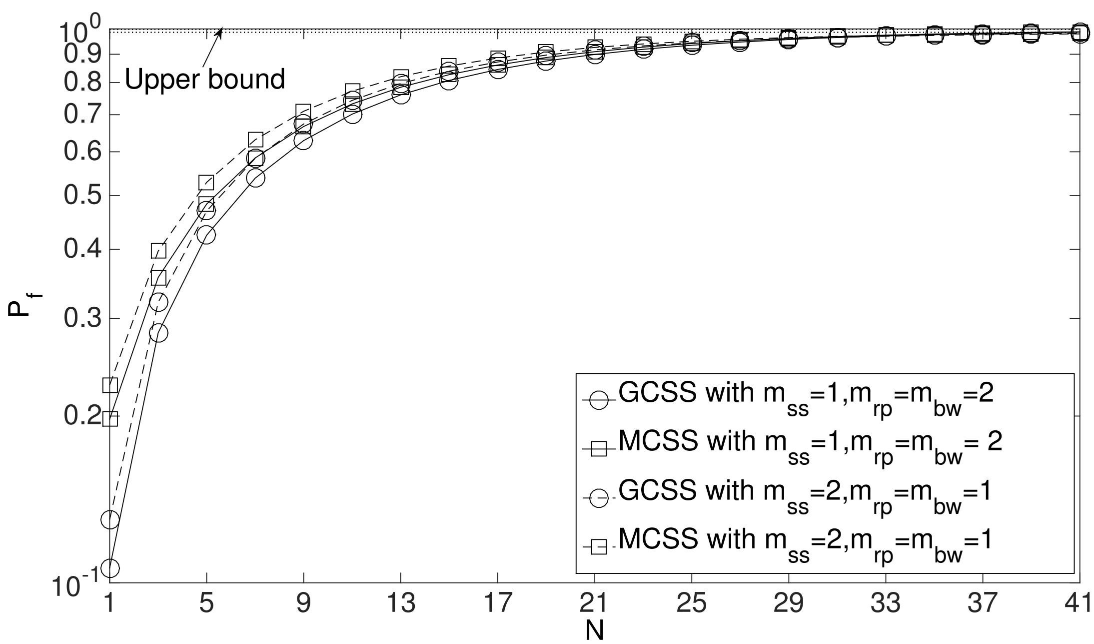

Fig. 4: FAP of CSS schemes over the number of SUs.

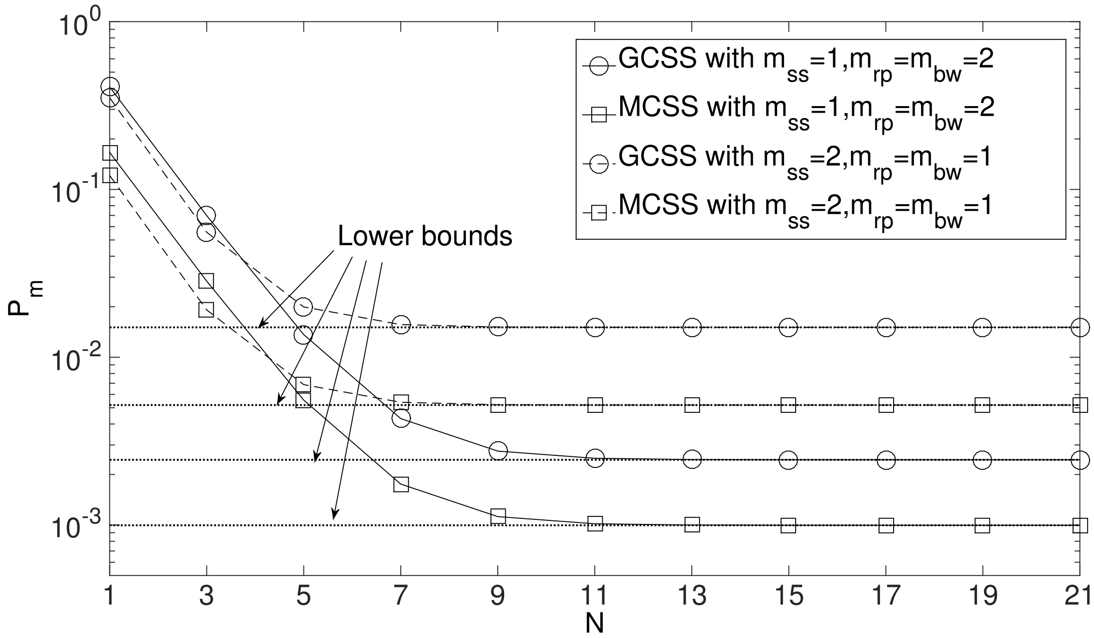

Fig. 5: MDP of CSS schemes over the number of SUs.

shown in Figs. 4 and 5 where the FAP and MDP of the two aforementioned CSS schemes are plotted as functions of N. The SNRs of the SS, RP and BW links are set as 8 dB, 10 dB and 12 dB, respectively. We consider two fading scenarios: i) $m_{ss} = 1$, $m_{rp} = m_{bw} = 2$, ii) $m_{ss} = 2$, $m_{rp} = m_{bw} = 1$ and iii) $m_{ss} = 1$, $m_{rp} = m_{bw} = 10$. It can be observed that both schemes approach the similar FAP upper bound as N is large, while the MDP of the MCSS scheme approaches a lower MDP bound. This accordingly verifies the statements in Remarks 2 and 4. Also, the FAP and MDP of the two CSS schemes are shown to approach the bounds given by (25), (26), (27) and (28) in Lemmas 4 and 5.

Fig. 6 plots the optimised number of SUs as a function of the SNR of SS links. Various fading scenarios are considered and the SNR of the RP and BW links are set as 6 and 4 dB, respectively. As shown in Lemma 6, N_{opt} is determined using numerical method with $\tau = 10^{-5}$ and 100 available SUs (i.e. $n_{\max} = 100$). It can be seen that a lower number of SUs can be

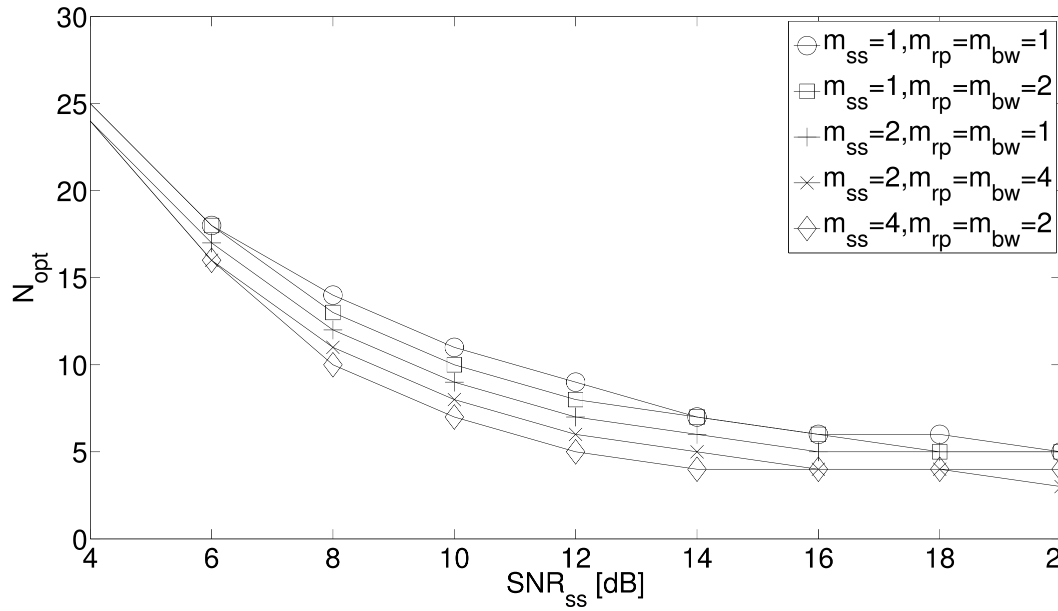

Fig. 6: Optimised Number of SUs over SNR of SS links.

selected to achieve the lower bound of the MDP rather than using all 100 SUs, which accordingly means a lower complexity and reduced power consumption are achieved with the proposed user selection for the CSS in CWRNs. Moreover, a lower N_{opt} is required as either the SS performance improves or the fading parameters increase.

VI. Conclusions

In this paper, we have analysed the MDP and FAP for two CSS schemes in CWRNs considering the practical scenario where all SS, RP and BW channels suffer from Nakagami-m fading. The derived expressions have shown the MCSS scheme achieves an improved MDP while causing a higher FAP when compared to the GCSS scheme. Both the MDP and FAP are improved as the fading parameters of the RP and BW channels increase, while the increased fading parameters of SS channels only results in a lower MDP. Furthermore, the bounds of the

MDP and FAP have been derived and an optimised number of SUs has been determined to reduce the complexity and power consumption in the CSS. For future work, we will investigate the performance of the CSS schemes along with the SU selection taking into account various scenarios of channel quality and node location.

REFERENCES

[1] S. Haykin, "Cognitive radio: brain-empowered wireless communications," *IEEE J. Sel. Areas Commun.*, vol. 23, no. 2, pp. 201–220, Feb. 2005.

[2] I. Mitola, J. and J. Maguire, G.Q., "Cognitive radio: Making software radios more personal," *IEEE Pers. Commun.*, vol. 6, no. 4, pp. 13–18, Aug. 1999.

[3] T. Yucek and H. Arslan, "A survey of spectrum sensing algorithms for cognitive radio applications," *IEEE Commun. Surveys and Tutorials*, vol. 11, no. 1, pp. 116–130, first quarter 2009.

[4] G. Ganesan and Y. Li, "Cooperative spectrum sensing in cognitive radio, part I: Two user networks," *IEEE Trans. Wireless Commun.*, vol. 6, no. 6, pp. 2204–2213, Jun. 2007.

[5] W. Zhang and K. Letaief, "Cooperative spectrum sensing with transmit and relay diversity in cognitive radio networks," *IEEE Trans. Wireless Commun.*, vol. 7, no. 12, pp. 4761–4766, Dec. 2008.

[6] K. Ben Letaief and W. Zhang, "Cooperative communications for cognitive radio networks," *Proc. of the IEEE*, vol. 97, no. 5, pp. 878–893, May 2009.

[7] G. Noh, H. Wang, J. Jo, B.-H. Kim, and D. Hong, "Reporting order control for fast primary detection in cooperative spectrum sensing," *IEEE Trans. Veh. Technol.*, vol. 60, no. 8, pp. 4058–4063, Oct. 2011.

[8] Y. Zou, Y.-D. Yao, and B. Zheng, "Cooperative relay techniques for cognitive radio systems: Spectrum sensing and secondary user transmissions," *IEEE Commun. Mag.*, vol. 50, no. 4, pp. 98–103, Apr. 2012.

[9] Q.-T. Vien, B. G. Stewart, H. Tianfield, and H. X. Nguyen, "Efficient cooperative spectrum sensing for three-hop cognitive wireless relay networks," *IET Commun.*, vol. 7, no. 2, pp. 119–127, 2013.

[10] M. Monemian and M. Mahdavi, "Sensing user selection based on energy constraints in cognitive radio networks," in *Proc. IEEE WCNC 2014*, Istanbul, Turkey, Apr. 2014, pp. 3379–3384.

[11] A. Cacciapuoti, I. Akyildiz, and L. Paura, "Correlation-aware user selection for cooperative spectrum sensing in cognitive radio ad hoc networks," *IEEE J. Sel. Areas Commun.*, vol. 30, no. 2, pp. 297–306, Feb. 2012.

[12] N. Hasan, W. Ejaz, S. Lee, and H. Kim, “Knapsack-based energy-efficient node selection scheme for cooperative spectrum sensing in cognitive radio sensor networks,” *IET Commun.*, vol. 6, no. 17, pp. 2998–3005, Nov. 2012.

[13] Y. Zhou, Z. Zhou, and B. Li, “Sensing nodes selection and data fusion in cooperative spectrum sensing,” *IET Commun.*, vol. 8, no. 13, pp. 2308–2314, Sep. 2014.

[14] M. Najimi, A. Ebrahimzadeh, S. Hosseini Andargoli, and A. Fallahi, “Energy-efficient sensor selection for cooperative spectrum sensing in the lack or partial information,” *IEEE Sensors J.*, vol. 15, no. 7, pp. 3807–3818, Jul. 2015.

[15] A. Ebrahimzadeh, M. Najimi, S. Andargoli, and A. Fallahi, “Sensor selection and optimal energy detection threshold for efficient cooperative spectrum sensing,” *IEEE Trans. Veh. Technol.*, vol. 64, no. 4, pp. 1565–1577, Apr. 2015.

[16] J. Ma, G. Zhao, and Y. Li, “Soft combination and detection for cooperative spectrum sensing in cognitive radio networks,” *IEEE Trans. Wireless Commun.*, vol. 7, no. 11, pp. 4502–4507, Nov. 2008.

[17] X. Liu and B. Sirkeci-Mergen, “Group-orthogonal MAC for cooperative spectrum sensing in cognitive radios,” in *Proc. IEEE MILCOM 2010*, San Jose, CA, USA, Oct. 2010, pp. 1221–1226.

[18] A. S. Cacciapuoti, M. Caleffi, L. Paura, and R. Savoia, “Decision maker approaches for cooperative spectrum sensing: Participate or not participate in sensing?” *IEEE Trans. Wireless Commun.*, vol. 12, no. 5, pp. 2445–2457, May 2013.

[19] F. F. Digham, M.-S. Alouini, and M. K. Simon, “On the energy detection of unknown signals over fading channels,” *IEEE Trans. Commun.*, vol. 55, no. 1, pp. 21–24, Jan. 2007.

[20] I. S. Gradshteyn and I. M. Ryzhik, *Table of Integrals, Series, and Products*, 7th ed. Academic Press, 2007.

[21] H. Shin and J. H. Lee, “On the error probability of binary and M-ary signals in Nakagami-m fading channels,” *IEEE Trans. Commun.*, vol. 52, no. 4, pp. 536–539, Apr. 2004.